

United States
Environmental Protection
Agency

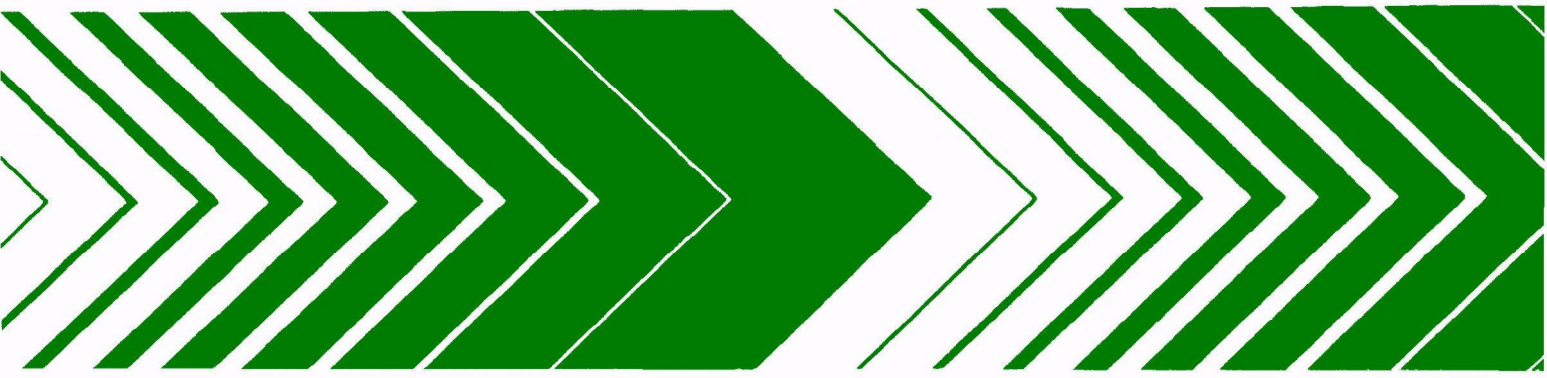
Environmental Sciences Research
Laboratory
Research Triangle Park NC 27711

EPA-600/3-80-018
January 1980

Research and Development



Mechanism of SO_2 and H_2SO_4 Aerosol Zinc Corrosion



RESEARCH REPORTING SERIES

Research reports of the Office of Research and Development, U.S. Environmental Protection Agency, have been grouped into nine series. These nine broad categories were established to facilitate further development and application of environmental technology. Elimination of traditional grouping was consciously planned to foster technology transfer and a maximum interface in related fields. The nine series are:

- 1 Environmental Health Effects Research
- 2 Environmental Protection Technology
- 3 Ecological Research
- 4 Environmental Monitoring
- 5 Socioeconomic Environmental Studies
- 6 Scientific and Technical Assessment Reports (STAR)
- 7 Interagency Energy-Environment Research and Development
- 8 "Special" Reports
- 9 Miscellaneous Reports

This report has been assigned to the ECOLOGICAL RESEARCH series. This series describes research on the effects of pollution on humans, plant and animal species, and materials. Problems are assessed for their long- and short-term influences. Investigations include formation, transport, and pathway studies to determine the fate of pollutants and their effects. This work provides the technical basis for setting standards to minimize undesirable changes in living organisms in the aquatic, terrestrial, and atmospheric environments.

This document is available to the public through the National Technical Information Service, Springfield, Virginia 22161.

MECHANISM OF SO_2 AND H_2SO_4 AEROSOL
ZINC CORROSION

by

Alan B. Harker
Florian B. Mansfeld
Dennis R. Strauss
Dwight D. Landis

Rockwell International Science Center
Thousand Oaks, CA 91360

Contract No. 68-02-2944

Project Officer

Fred Haynie
Environmental Sciences Research Laboratory
Research Triangle Park, N.C. 27711

ENVIRONMENTAL SCIENCES RESEARCH LABORATORY
OFFICE OF RESEARCH AND DEVELOPMENT
U.S. ENVIRONMENTAL PROTECTION AGENCY
RESEARCH TRIANGLE PARK, N.C. 27711

DISCLAIMER

This report has been reviewed by the Environmental Sciences Research Laboratory, U.S. Environmental Protection Agency, and approved for publication. Approval does not signify that the contents necessarily reflect the views and policies of the U.S. Environmental Protection Agency, nor does mention of trade names or commercial products constitute endorsement or recommendation for use.

ABSTRACT

A twelve-month experimental study has been conducted to establish the physical variables controlling the SO_2 (gas) and H_2SO_4 (aerosol) induced corrosion of zinc. The study was carried out using a 6.6 m aerosol flow reactor in which relative humidity, temperature, air flow velocity, flow turbulence, aerosol size range, and pollutant concentration were controlled. Corrosion measurements were made through the use of an atmospheric corrosion monitor previously developed in this laboratory. The results of the study showed that the principal factors controlling pollutant induced corrosion are relative humidity (time of surface wetness), the rate of pollutant flux to the surface, and the chemical form of the pollutant, while temperature was not observed to be a controlling factor within the experimental range (12 to 20°C). SO_2 was observed to induce a higher corrosion rate in the zinc than H_2SO_4 on a molecule for molecule basis. Flow dynamic measurements provided bulk and size detailed deposition velocities for two different accumulation mode H_2SO_4 aerosol size distributions as a function of frictional velocity, and a deposition velocity for SO_2 gas. The overall results indicate that under most ambient conditions SO_2 induced corrosion damage will dominate over H_2SO_4 effects. This study demonstrated the capability of the experimental technique to observe the physical and chemical processes controlling pollutant induced corrosion and offers a means of quantitatively describing these effects through further investigation.

This report was submitted in fulfillment of (contract No. 68-02-2944) by (Rockwell International Science Center) under the sponsorship of the U.S. Environmental Protection Agency. This report covers a period from 5/9/78 to 6/9/79, and work was completed as of 6/9/79.

CONTENTS

Abstract	iii
Figures	vi
Tables	vii
1. Introduction	1
2. Experimental	4
Aerosol flow system	4
Gas/aerosol flow generation	4
Turbulent flow development	6
Test section	8
Experimental approach	10
3. Results	12
Flow dynamic measurements	12
Aerosol size distribution	15
Deposition velocity determination	15
Corrosion measurements	20
High-low condition tests	23
NH ₄ HSO ₄ aerosol generation	25
Corrosion chemistry	25
4. Discussion of Results	30
References	32

FIGURES

<u>Number</u>		<u>Page</u>
1	Size distribution of atmospheric particles ⁽⁴⁾	2
2	Aerosol flow system	5
3	Aerosol generation system	7
4	Atmospheric corrosion monitor	9
5	Velocity profiles observed as a function of the distance from the wall for the smooth tube and the tube with per- turbance barriers 20 cm from the ACM position. ($R=R_0$ at the wall	13
6	H ₂ SO ₄ aerosol particle size and mass distribution without the cyclone separator in the flow stream	16
7	H ₂ SO ₄ aerosol particle size and mass distribution with cyclone separator in the flow system	17
8	Ratio of integrated XPS S _{2p} signal to integrated XPS Zn _{2p} signal for H ₂ SO ₄ -treated Zn discs (0.242 cm ² surface area)	21
9	Comparison of experimental aerosol deposition velocities with those predicted by Sehmel (9), for a frictional velo- city of 35 cm/sec	22
10	Comparison of the humidity response of the atmospheric corrosion monitor with various surface pre-treatments	24
11	Output current of atmospheric corrosion monitor as a function of SO ₂ concentration	26
12	Comparison of observed ACM current response to H ₂ SO ₄ aerosol deposition at two frictional velocities. H ₂ SO ₄ concentration = 3.2 mg/m ³	27

TABLES

<u>Number</u>		<u>Page</u>
1	Frictional velocities and roughness heights.	14
2	Experimental H_2SO_4 aerosol deposition velocities.	19

SECTION 1

INTRODUCTION

The degradation of materials through corrosion, accelerated by airborne gaseous and particulate pollutants, is one of the major economic effects of the increase in atmospheric pollution in urban areas. Primary concern in this area is focused upon the role of sulfur species in the corrosion process due to the increased use of high sulfur fuel oil and coal fuels in power generation. This twelve-month laboratory study was conducted to provide kinetic data required to develop a materials damage model to describe the effects of pollutants upon atmospheric corrosion rates.

Industrial sources by far supply the bulk of pollutant sulfur in the urban United States, with the sulfur being primarily in the form of gaseous SO_2 with only about 1.25% of the sulfur being produced as H_2SO_4 mist.⁽¹⁾ However, by direct and indirect photochemical as well as heterogeneous oxidation processes, the gaseous SO_2 is converted to sulfates and incorporated into atmospheric aerosols. The chemical form of the sulfate is to a large extent controlled by the age of the aerosols and the gaseous concentrations of neutralizing species such as ammonia. Newly-formed sulfate aerosols, either from a primary source or from photochemical oxidation of SO_2 , are principally H_2SO_4 , while aged aerosols have a greater sulfate salt content with ammonium salts dominating.⁽²⁾ Urban sulfate levels in the United States are regional; however, levels from 3 to 25 $\mu\text{g}/\text{m}^3$ are typical except during episode conditions, where levels of 80 $\mu\text{g}/\text{m}^3$ and higher are reached.⁽³⁾

The size distribution of sulfate in aerosols determines the mechanism by which they reach the surface of materials. Typically, ambient aerosols have a size distribution similar to that shown in Fig. 1⁽⁴⁾ with three distinct particle size modes; the Aitken nuclei, accumulation range, and mechanically generated particles. The bulk of aerosol sulfates (over 80%) is associated with the accumulation mode aerosols - those particles with diameters between 0.1 and 1.0 micron.⁽⁵⁾ These accumulation mode aerosols, formed primarily from coagulation of and condensation on Aitken nuclei, are those with which this study is concerned. This size range of aerosols is primarily removed from the atmosphere by dry deposition on surfaces, incorporation into cloud droplets (rainout), and removal by falling precipitation (washout).

Electrochemical corrosion occurs when pollutant sulfur species are deposited on wet metal surfaces. Typically, surfaces are wet from condensation rather than precipitation, with condensation occurring when the relative humidity adjacent to the surface exceeds the equilibrium value for a saturated solution of the corrosion products or hygroscopic contaminants on the

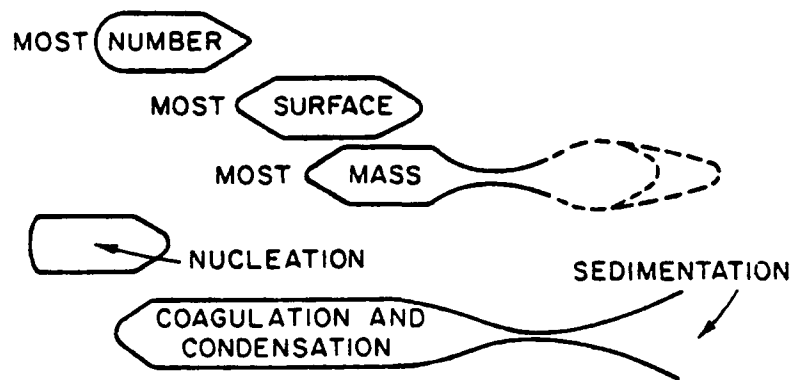
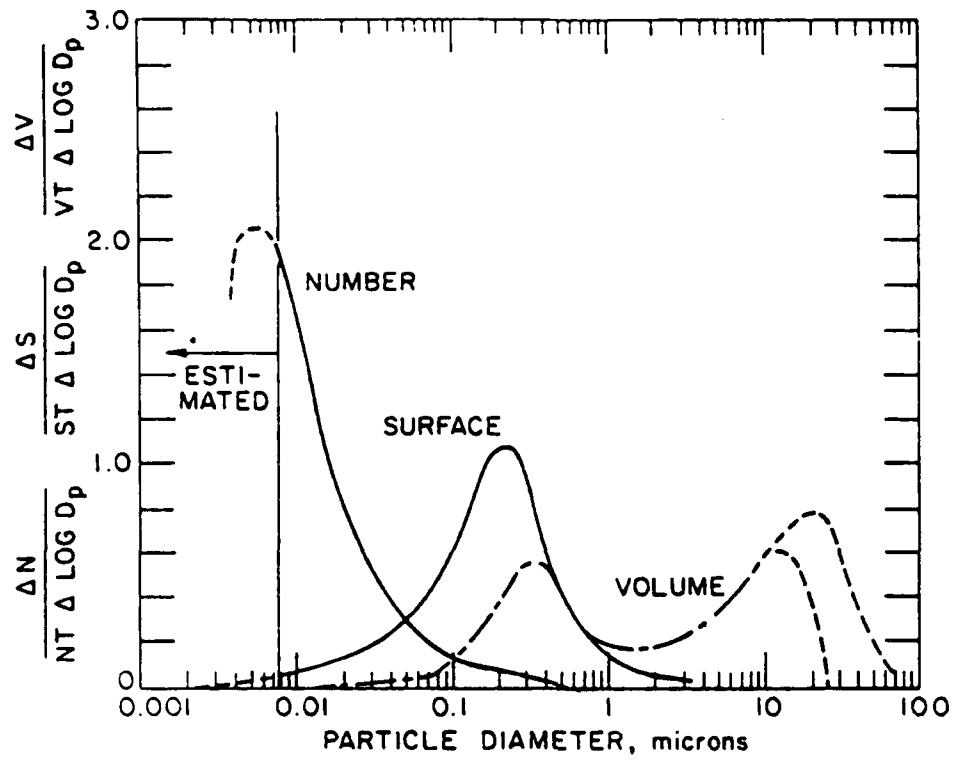


Figure 1. Size distribution of atmospheric particles.⁽⁴⁾

surface. When the sulfur pollutants react with a surface, they can increase the rate of corrosion through a number of processes. The initial chemical reaction itself damages the outer passivated surface of the material and the products formed can be hygroscopic which will increase the time of wetness of the corroding surface. The reaction products can also increase the corrosion rate by making the surface water layer more conductive and they can participate in corrosion reactions as catalytic reaction intermediates. The presence of acid pollutants also lowers the pH of the surface solution and increases the solubility of the corrosion products.

In this investigation, research was carried out to determine the physical variables controlling the corrosion rate of zinc caused by exposure to gaseous sulfur dioxide (SO_2) and aerosol particles containing sulfates in the form of H_2SO_4 and NH_4HSO_4 . To provide the necessary experimental control for observation of the corrosion process and to determine the rates of deposition of both gaseous and particulate sulfur pollutants, an aerosol flow reactor was designed and developed specifically for this investigation. This apparatus described in the next section provides a fully developed turbulent air flow at a constant velocity, temperature, and relative humidity in which both SO_2 and sulfate aerosols can be supplied to a test section containing flow dynamic, aerosol, and corrosion monitoring instrumentation. The corrosion measurements were made through the use of an atmospheric corrosion monitor (ACM) developed at the Science Center by F. Mansfeld and co-workers.⁽⁶⁻⁷⁾ The variables found to have the greatest effect upon the corrosion process were relative humidity, pollutant concentration, wind frictional velocity, and aerosol size range. The direct relationship observed between the flow dynamic parameters and the corrosion rates supports the hypothesis that the corrosion process was limited by flux of pollutants to the surface.

SECTION 2

EXPERIMENTAL

AEROSOL FLOW SYSTEM

The flow reactor, designed and constructed during this program, is shown schematically in Figure 2. The flow reactor was constructed in a 12'x20' steel shed under the Science Center so that the main air supply system of the building could be utilized to provide a high flow volume of conditioned air and so that exhausting the test air would provide no health problems. The flow system had four main sections; the gas/aerosol flow generation section, the turbulent flow development pipe, the experimental test section, and the aerosol scrubber and exhaust assembly. These sections will be described in detail in the following.

GAS/AEROSOL FLOW GENERATION

The air inlet to the flow system as shown in Figure 2 was attached to the main air conditioning supply for the laboratory with a high pressure blower pushing the required 0.5 to 8.5 m³/min of air through the experimental system. The air flow rate is controlled by an adjustable damper mounted on the blower inlet and can be regulated at average flow velocities from 0.5 to 8 m sec⁻¹. The average flow velocity was continuously monitored at the inlet to the turbulent flow development pipe section by a pitot tube, and the absolute flow velocity profile was determined across the diameter of the pipe by a Thermosystems model 1610-2 velocity probe in the test section.

In the 30x30 cm ducting bringing the air into the blower are mounted two water aerosol generators and six 500 watt radiant heaters to provide initial humidity and temperature control. The flow rate through the water aerosol generators can be controlled and the heaters can be individually turned on or off. Two additional 600 watt heater units and a third water aerosol generator were placed after the blower unit to provide further humidity control. The entire ducting system was wrapped in 6-inch batts of fiberglass insulation to provide temperature stability.

Through the thermostatic control on the laboratory air conditioning supply and the eight separate radiant heaters, it is possible to control the air temperature in the flow system over the range 12 to 28°C with a temperature drift of less than ±0.5°C per hour. The relative humidity can be controlled over the range 30 to 90% RH with stability of ±0.5% RH per hour. At RH levels above 95% small fluctuations could cause rainout to occur in the flow lines, hence RH values in the main pipe section were kept below 90%. In the test section higher RH values were obtained by cooling the surface of

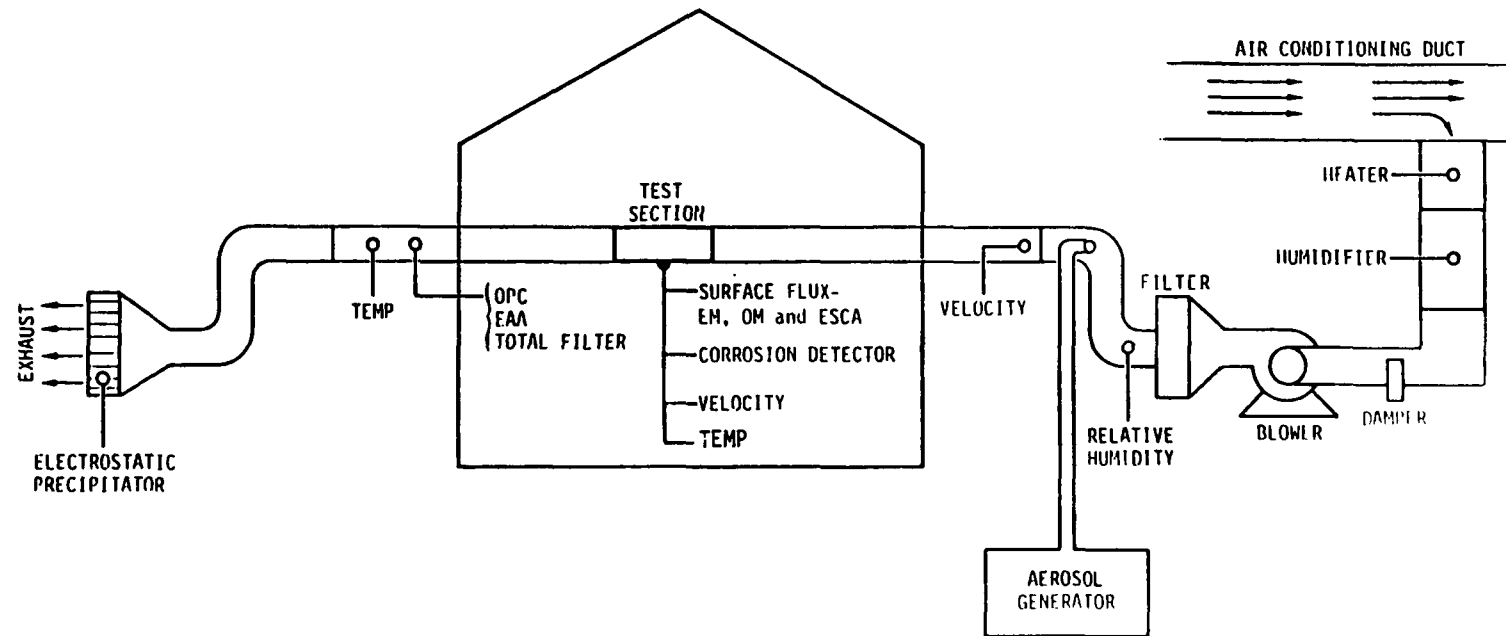


Figure 2. Aerosol flow system.

the corrosion monitor by pumping refrigerated water through cooling lines wrapped around the ACM base.

After the humidifying section the air was passed through a high efficiency HEPA filter to remove any water aerosols and particulates in the air. The conditioned air exiting from the HEPA filter then passed into a section of ducting containing the mixing ports for test aerosols and gaseous SO_2 as well as a Phys. Chemical Corp. Humeter, a Pitot flow meter, and air temperature monitoring thermistor.

The SO_2 for the experiments was from a 0.5% Matheson Certified Standard mixture of SO_2 in Ultra High Purity nitrogen. The gas was metered into the main air flow through a calibrated rotameter.

The test aerosols were produced by an Environmental Research Corp. Model 7330 Fluid Atomization Aerosol Generator. The atomizer source provides a poly-disperse aerosol distribution with a mean diameter of about 0.05 micron. To provide larger aerosols with a narrower distribution, the output of the atomizer was passed into a 22 liter cylindrical glass reservoir with a residence time of 3 minutes as shown in Figure 3. The reservoir provided enough time for the aerosols to coagulate into the accumulation mode with the resulting size distribution having a mean diameter of about 0.2 microns. The output from the aerosol reservoir was passed through a cyclone separator designed to remove particles with an aerodynamic diameter greater than 1 micron, and then into a beta radiation source to remove any residual static charge the particles may have developed in the flow system. The particles were mixed with the main flow stream to the apparatus at the outlet of the HEPA filter.

The aerosol size distribution, total mass and number concentration were the subject of extensive analysis with measurements being taken by three types of particle analyzers and through microscopic examination of filter samples. The aerosol analyzers used in the experiments were a TSI Model 3030 Electrical Aerosol Analyzer, a Royco Optical Particle Counter and a California Measurements Corp. Model C1004 Cascade Impactor equipped with Piezo-electric microbalance particle mass monitors. Total mass concentration and deposition rates were determined by weighing collected filters on a Cahn microbalance and deposition rates were measured by transmission microscopic examination of samples collected on TEM analysis grids and XPS analysis of zinc samples. The results of these aerosol analyses will be discussed in detail in the results section.

TURBULENT FLOW DEVELOPMENT

After passing through the HEPA filter and being mixed with the aerosol flow, the air enters a 3.3 meter section of smooth 16.7 cm ID PVC pipe. In this flow length (about 20 pipe diameters) turbulent flow is developed for all velocities in excess of 0.2 m/sec using the Reynolds equation for critical velocities in a smooth pipe to describe the flow. To increase the air-flow turbulence and give a range of frictional velocities for the experiments perturbation barriers were placed in the pipe in some of the experiments. The perturbances are 2 cm high Teflon rings with 1 cm square serrations cut into

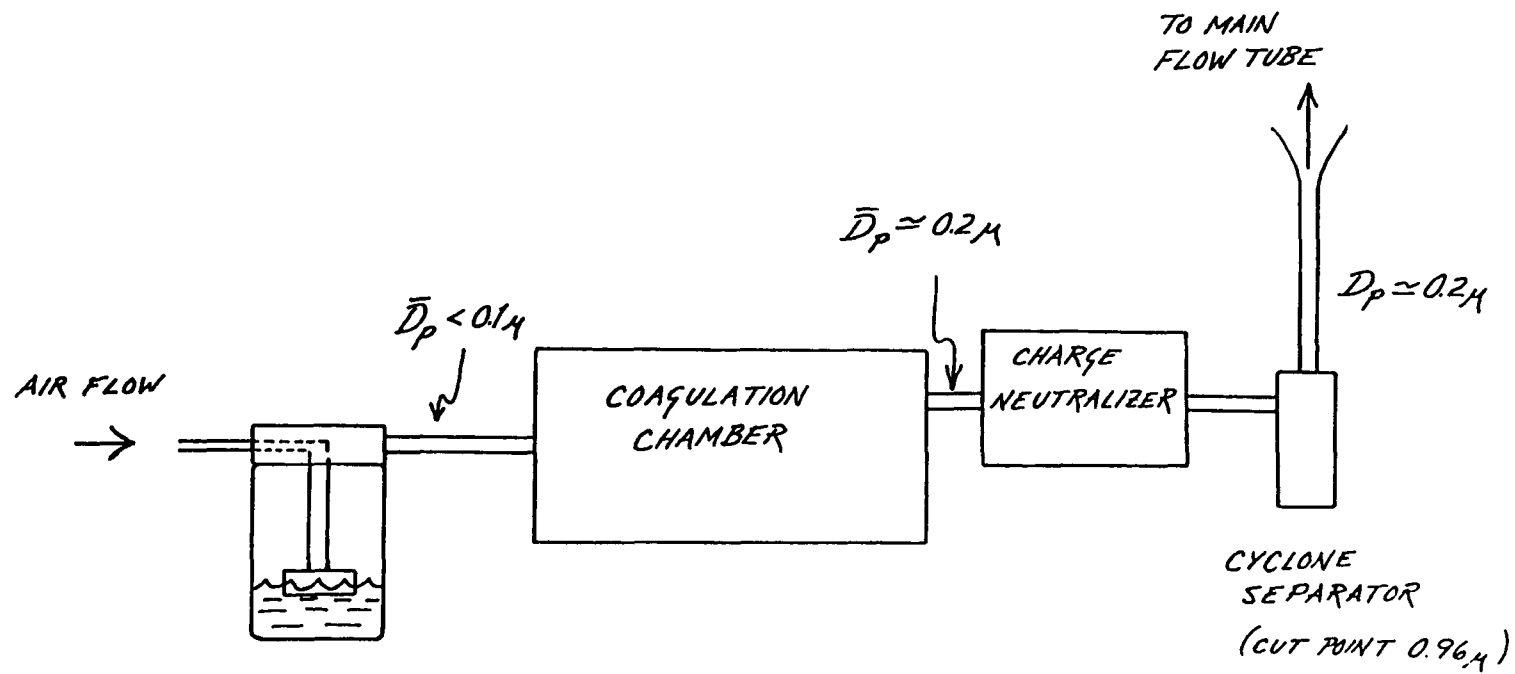


Figure 3. Aerosol generation system.

them. Up to three rings were used in the system with the serrations offset to create maximum turbulence. The rings were spaced 6 cm apart and were placed at distances varying from 2 to 20 cm upstream from the corrosion monitor.

TEST SECTION

The test section of the apparatus is a removable aluminum pipe (60 cm length, 16.4 cm O.D., 15.2 cm I.D.) which is inserted into and joins the two longer sections of PVC pipe. O-ring-sealed ports in this section accommodate velocity, temperature, aerosol, and corrosion monitoring detectors. The test section is well grounded to reduce surface charging and prevent electrostatic deposition of aerosol particles. It is wrapped with heating tape and insulated with fiberglass batting. A YSI Model 72 temperature controller maintains constant wall temperature by controlling the current through the heating tape.

Corrosion measurements were made in the test section through the use of the atmospheric corrosion monitor (ACM) developed at the Science Center by Mansfeld and co-workers^(6,7). The ACM was made up of twenty 0.62 mm zinc plates separated by 0.025 mm Mylar film with alternate plates electrically connected to make a capacitor circuit as shown in Figure 4. The assembly was potted in epoxy and machined to fit into a gas-tight opening in the test section. The ACM was AC biased to ± 30 mv at a 1 cycle per minute while the resulting current was continuously monitored. The temperature of the ACM was controlled by the heating unit on the test section and cooling coils carrying water from a Haake refrigeration system wrapped around the ACM's base. With this cooling capability, the ACM's temperature, as recorded by a thermistor, could be kept slightly lower than the air temperature to induce condensation on the surface, if desired.

The YSI model 1610-2 velocity probe can be inserted into the test section through either of two 90 degree offset, o-ring sealed ports and translated across the pipe to provide flow velocity profiles.

The test section is also fitted with o-ring mounted electron microscope sample grid stages. These stages are flush to the wall of the pipe and introduce minimal flow disturbance. Transmission electron microscope aerosol collection grids and zinc x-ray photoelectron spectroscopy samples were mounted on these stages with silver paint.

Following the test section the flow pipe extends another 3.3 meters to prevent interruption of the turbulent flow. Aerosol sample ports were machined into the walls of this section to provide a continuous flow of aerosols for the aerosol monitoring equipment and total filter collection.

At the end of this section the flow stream passes through a commercial electrostatic precipitator to remove the sulfate aerosols before venting to the ambient air.

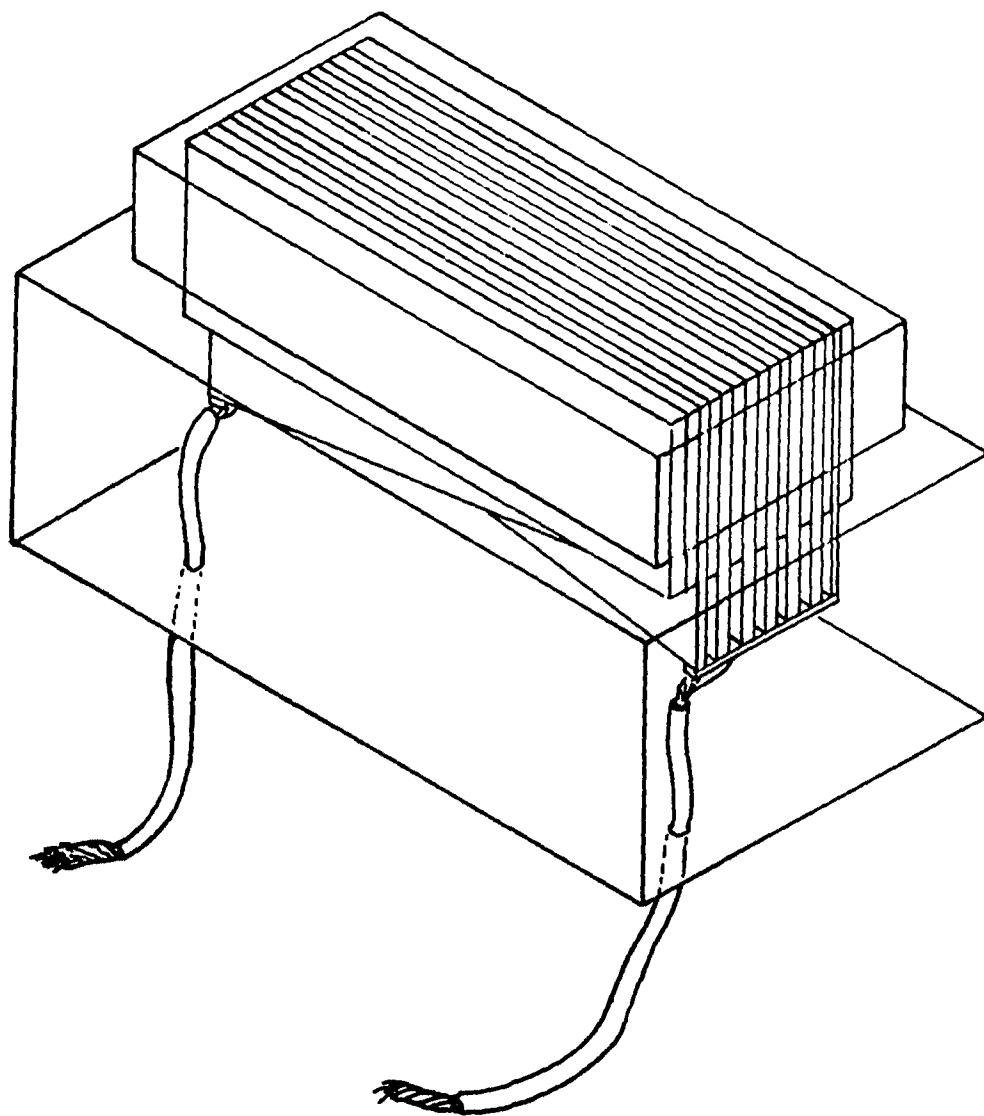


Figure 4. Atmospheric corrosion monitor.

EXPERIMENTAL APPROACH

The nature and number of the experimental measurements being made during each test run required that the flow system be maintained in a steady-state with respect to flow rate, relative humidity, and aerosol concentration for periods of 4 to 8 hours duration. To obtain this stability was difficult, due to the high volume of air being passed through the system; however, as experience was gained with the technique, the required stability of operation was achieved. With steady-state conditions established, the following measurements were performed for each complete test.

I) Environmental Measurements

- a) % RH and temperature monitored in two points
- b) Average flow velocity (Pitot tube)
- c) Flow velocity profile recorded when steady-state established

II) Aerosol Measurements

- a) Aerosol size distribution and number concentration determined at intervals during test by TSI 3030 analyzer.
- b) 2 total mass filter samples were collected
- c) TEM deposition grid samples collected continuously
- d) X-ray photoelectron spectroscopy samples (both zinc plate and aluminum foil) collected continuously during experiment.

III) Corrosion Rate Measurements were recorded continuously from the ACM detector throughout each experiment.

Typically experimental conditions were selected over the following ranges for the controllable variables.

Temperature	12 - 20 C
% RH	65 - 100%
Average Flow Velocity	0.5 - 8 m/s
SO ₂ concentration	- 46 to 216 ppb by volume
SO ₄	= aerosol mass concentration 1.2 mg/m ³
Aerosol size distribution	0.01 - 1.0 micron diameter
ACM pretreated with	0.1 N H ₂ SO ₄ or NH ₄ HSO ₄

The experimental procedure consisted of running the flow apparatus with only humidified air to establish a steady-state RH and temperature and to obtain a background current from the ACM. Upon obtaining a stable background, SO₂ would be introduced to the gas flow and the ACM response recorded over a two-hour period at which time the SO₂ would be turned off and the ACM allowed to again reach a stable baseline. With a baseline again established, aerosols would be introduced into the flow and continued for 2 to 4 hours.

At the completion of a test, the total filter samples, TEM grids, and XPS samples would be removed from the test section and analyzed by the appropriate techniques.

SECTION 3

RESULTS

The data from the flow dynamics, aerosol characterization, and corrosion measurements will be discussed separately with the combined results being treated later in this report.

FLOW DYNAMIC MEASUREMENTS

The initial concern in the design of the experimental apparatus was to provide a well-characterized turbulent air flow to the measurement section. Hence a long flow tube was utilized (6.6 meters) providing 22 diameters of length both before and after the test section, and in all test cases the air flow velocity was set above the critical velocity for turbulent flow (0.2 m/sec at 20°C) which is defined as:

$$V_{crit} = \frac{2000 \nu}{d} \quad (I)$$

In this expression, ν is the kinematic coefficient of viscosity ($1.5 \times 10^{-5} \text{ m}^2 \text{ sec}^{-1}$ for air at 20°C) and d is the pipe diameter. (8)

The extent of the turbulence in the pipe is a function of the resistance of the pipe wall to the flow. As the friction between the flowing material and the pipe wall is increased (due to surface roughness or barriers) the turbulence increases. This effect was observed in the experimental apparatus by placing the serrated barriers described in the experimental section in the pipe. Figure 5 shows two velocity profiles, one taken at 3.96 m/sec in the smooth pipe, the other taken at 4.65 m/sec in the pipe with 3 barriers in place, the closest one 21 cm from the test point.

To provide a measure of the turbulence, "frictional velocity" and "roughness height" are defined for the flow. The frictional velocity (ν^*) is related to the velocity profile by the expression

$$V(y) = \frac{\nu^*}{K^+} \ln \left(\frac{y+y_0}{y_0} \right) \quad (II)$$

where $V(y)$ is the observed velocity at distance y from the pipe wall, K^+ is Von Karman's constant (0.417, ref 9) and y_0 is the roughness height of the pipe. The frictional velocity and roughness height parameters were obtained for the flow conditions of the test runs by carrying out a least squares fit of the observed velocity profiles to equation (II). As the results in Table 1 show, frictional velocities of 3.5 to 75 cm/sec were obtained in the flow system with roughness heights of $< 10^{-3}$ cm and ~ 0.2 cm respectively. The correlation coefficients for the fit of the observed data to eq (II) were

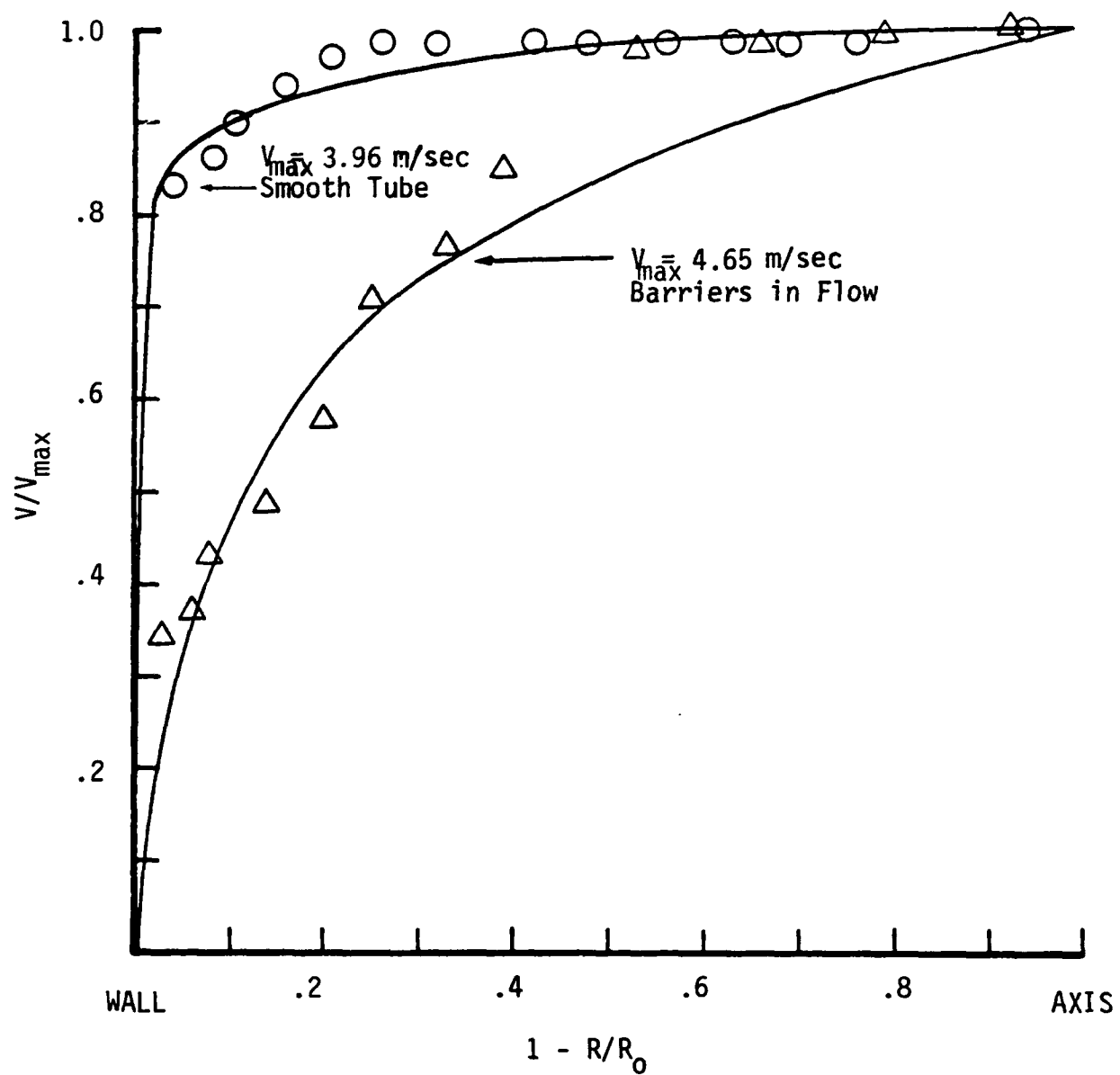


Figure 5. Velocity profiles observed as a function of the distance from the wall for the smooth tube and the tube with perturbation barriers 20 cm from the ACM position. ($R = R_0$ at the wall)

TABLE 1. FRICTIONAL VELOCITIES AND ROUGHNESS HEIGHTS OF SMOOTH FLOW TUBE AND TUBE WITH THREE SERRATED PERTURBANCES PLACED IN FLOW WITH THE FIRST PERTURBANCE BARRIER 20 CM FROM THE TEST POSITION. TABULATED VALUES ARE FROM A LEAST SQUARES FIT OF THE EXPERIMENTAL VELOCITY PROFILE DATA TO EQUATION (II).

Maximum Flow Velocity V_{\max} (cm/sec)	Frictional Velocity ν^* (cm/sec)	Roughness Height Y_0 (cm)	Correlation Coefficient r^2
(Smooth Pipe) 146	3.5	$< 10^{-3}$	0.93
238	8.6	$< 10^{-3}$	0.94
305	9.1	$< 10^{-3}$	0.95
760	22.3	$< 10^{-3}$	0.96
1,036	39.3	$< 10^{-3}$	0.92
(Barrier in flow) 700	75	0.16	0.82
425	50	0.26	0.87
289	33.8	0.21	0.81
155	18.8	0.18	0.97

typically around 0.94 for the smooth pipe flow and between 0.80 to 0.90 for the tests with the perturbation barriers in place. The fit between equation (II) and the velocity profile data is shown in Figure 5 where the solid curves are those predicted by the least squares fitting procedures.

AEROSOL SIZE DISTRIBUTION

The sulfate aerosols produced by the ERC fluid atomization aerosol generator were monitored by a number of aerosol analyzers during the experimental program to provide a size distribution and number concentration for the airborne particulates. The H_2SO_4 aerosol size distribution of the direct output of the ERC aerosol generator, as determined by the Thermosystems Electrical Aerosol Analyzer (EAA) and CMC Model C1004 Cascade Impactor (PPM), showed about 90% of the particles to be below 0.1 micron in diameter with only a small portion of the particles having diameters as great as 1 μ . Since accumulation mode aerosols are typically 0.1 μ to 1.0 μ in diameter, a 22 liter coagulation chamber was added to increase the size of the small particles. Figure 6 shows the effect of the addition of the coagulation chamber as determined by EAA and PPM analysis. The particle size and mass distribution data show the maximum of the number distribution to occur at 0.17 to 0.2 microns diameter with > 90% of the particles being in the accumulation mode size range. Assuming the aerosol particles to be spherical, a mass concentration distribution can be calculated and this is shown by the filled circles in Figure 6 for the aerosol from the coagulation chamber. As can be seen, the mass maximum is at 0.6 micron with a significant portion of the aerosol mass being contained in the particles with diameters greater than 1.0 micron. To reduce the mass contribution of the particles of > 1 μ diameter a cyclone separator was included in the aerosol flow system after the coagulation chamber. The cyclone separator was designed to have a 50% cut point at 0.96 μm for a flow rate of 1.0 scfm. The result of adding the cyclone is shown in Figure 7. The maximum of the number concentration is at 0.2 microns with the maximum mass concentration occurring at 0.4 microns. For this distribution particles of diameter greater than 1 micron comprise less than 10% of the total mass. The cyclone also lowers the total number concentration significantly, bringing the total aerosol mass down about a factor of five from the case without the separator.

To obtain gravimetric determinations of the total aerosol mass, known volumes of air from the flow system were passed through preweighed Millipore Spectro Grade A glass fiber filters for particle collection. The collected samples were weighed on a Cahn microbalance at known humidity to determine the aerosol mass.

DEPOSITION VELOCITY DETERMINATION

The deposition velocity K of gaseous and particulate pollutants is defined by the relationship

$$K = \frac{\text{amount deposited/cm}^2 \text{ of surface-sec}}{\text{airborne particle concentration above the surface}} \quad (\text{III})$$

This deposition velocity results from the combined effect of all the pro-

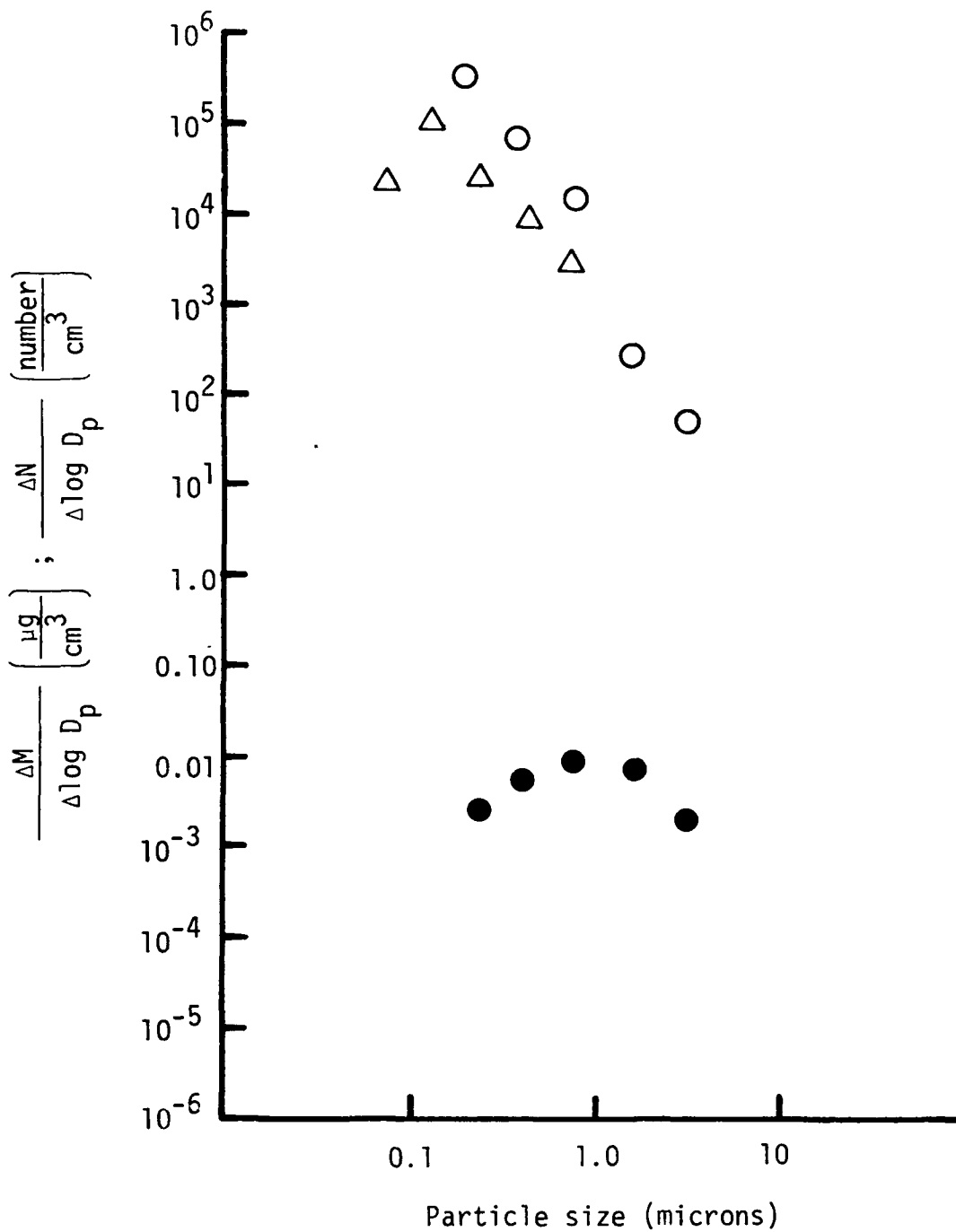


Figure 6. H_2SO_4 particle number and mass distribution without cyclone separator in the flow stream.

- △ - Electrostatic Aerosol Analyzer
 - - Piezoelectric Particle Monitor
 - - Mass Distribution
- } Number Distribution

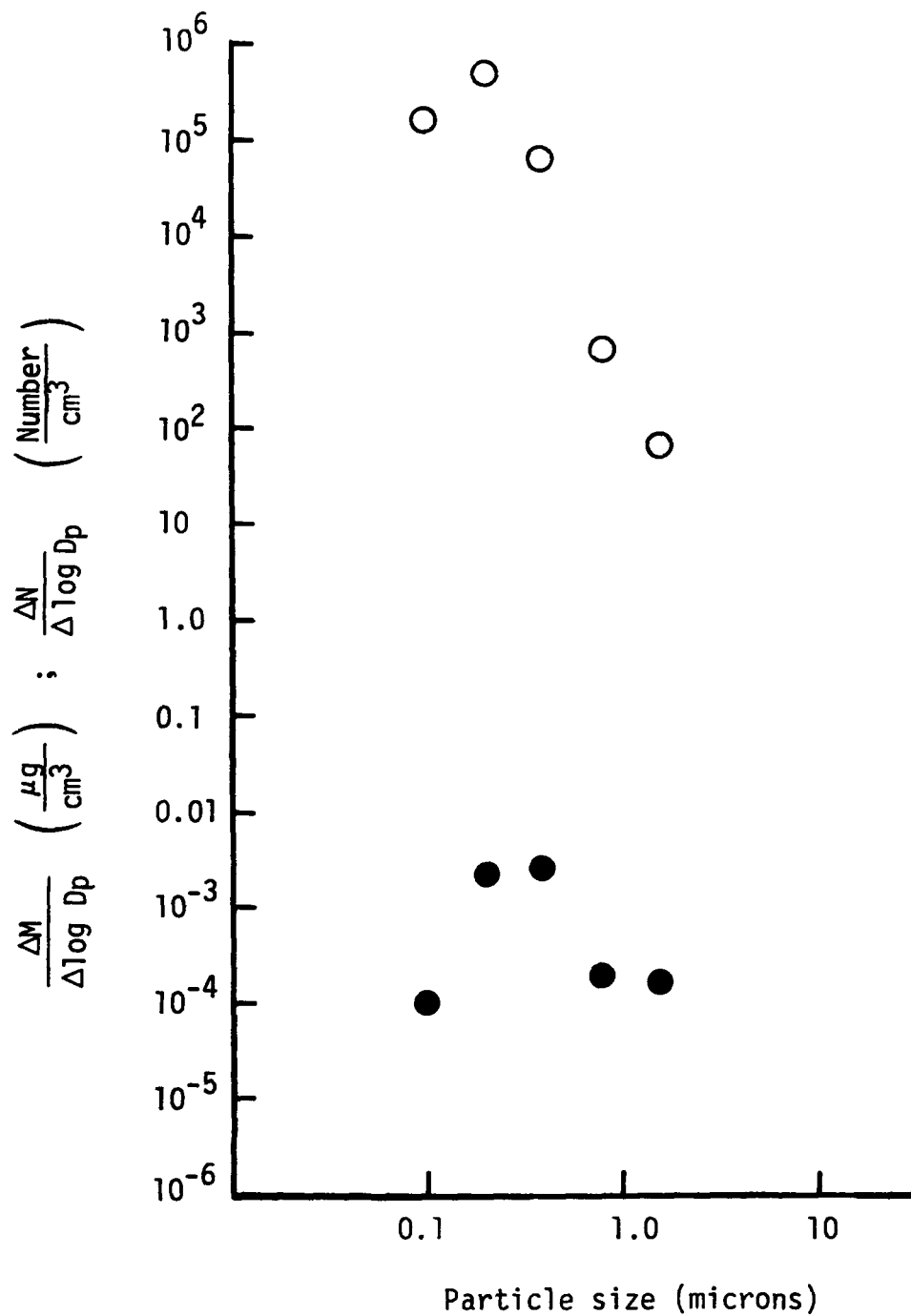


Figure 7. H_2SO_4 aerosol particle number and mass distribution with cyclone separator in the flow system.

○ - Number Distribution

● - Mass Distribution

cesses contributing to deposition. To determine this value for the aerosol and gaseous sulfur species in this study a combination of spectroscopic and gravimetric measurements was used.

The flux of aerosols depositing onto the ACM surface at the bottom of the flow reactor was observed by two methods; analyzing deposited samples with a transmission electron microscope (TEM) and carrying out x-ray photoelectron spectroscopy (XPS) analyses of sulfate deposition on zinc discs. Gaseous SO₂ deposition was also characterized by XPS sulfate analyses.

The TEM measurements used an instrument equipped with a computer automated program for particle counting and sizing on standard grids. In the experimental test section, graphite-coated TEM sample grids were mounted in the plane of the ACM detector (bottom of the flow tube). After each test run the grids were Pt-Pd coated at a fixed 30 degree deposition angle for study in the TEM. The use of angular Pt-Pd deposition produces a "shadow" of the individual particles which can be seen by the TEM to aid in calculating particle volumes. The primary goal of the TEM analyses was to establish the dependence of the deposition velocities on the diameter of the aerosol particles and the frictional velocity of the flow system. Due to the complexity of the analysis procedures TEM samples were not obtained over the range of conditions used in this study. However, for the case of H₂SO₄ aerosols deposited at frictional velocities of about 35 cm/sec, adequate data was obtained to describe the deposition velocities for the two aerosol distributions shown in Figures 6 and 7.

The particle size dependence of the deposition velocities was calculated from the TEM data by determining the total particle mass in each incremental size range per unit area on the collection surface and dividing by the collection time and the corresponding airborne aerosol mass as shown by,

$$K_{Dp} = \frac{(\text{Aerosol mass per unit area on surface in size range } D_p)}{(\text{Aerosol mass airborne per unit volume in size range } D_p)} / \text{sec} \quad (\text{IV})$$

The total mass of aerosol particles observed on the surface and total airborne aerosol mass can also be used with equation (III) to calculate a bulk deposition velocity for the aerosol distribution. The TEM data from three similar test runs for the aerosol distribution formed with the cyclone separator (Fig. 7) were used to calculate the K_{Dp} at a flow velocity of $V_{\max} = 305$ cm/sec with the barriers in the flow ($v^* = 35$ cm/sec). Two similar test runs were combined for the case with the cyclone separator removed from the flow system (Fig. 6) again at $V_{\max} = 305$ cm/sec and $v^* = 35$ cm/sec. The calculated values for K and K_{Dp} for these distributions are shown in Table 2. The bulk deposition velocity for the aerosol distribution without the cyclone is significantly larger due to the contribution of the larger particles.

The XPS analyses of collected aerosol particles provided a second means of determining the bulk deposition velocities. This was accomplished by comparing the sulfur signal amplitude observed on 7/32 inch zinc discs mounted in the flow tube with sulfate standards prepared by spraying polished Zn discs with 1.0 μ l aliquots of dilute H₂SO₄ solutions of known concentration (0.0028M to 0.028M). The samples were allowed to dry overnight in room air, then

TABLE 2. AEROSOL DEPOSITION VELOCITIES DETERMINED FROM XPS AND TEM ANALYSES FOR THE TWO EXPERIMENTAL ACCUMULATION MODE PARTICLE SIZE DISTRIBUTIONS.

DISTRIBUTION I - FIG. 6 (NO CYCLONE SEPARATOR)

DISTRIBUTION II - FIG. 7 (CYCLONE SEPARATOR IN FLOW)

Deposition Velocities From XPS Measurements

Aerosol Distribution I

$$K_{H_2SO_4} = 0.07 \pm 0.02 \text{ (cm/sec) for } V_{\max} = 305 \text{ (cm/sec)}$$

$$\nu^* = 35 \text{ (cm/sec)}$$

$$K_{H_2SO_4} = 0.10 \pm 0.04 \text{ (cm/sec) for } V_{\max} = 700 \text{ (cm/sec)}$$

$$\nu^* = 75 \text{ (cm/sec)}$$

Gaseous SO_2

$$K_{SO_4} = 0.93 \pm 0.2 \text{ (cm/sec) } V_{\max} = 400 \text{ (cm/sec)}$$

$$\nu^* = 50 \text{ (cm/sec)}$$

Deposition Velocities From TEM Measurements

Due to the small surface area examined in each TEM analysis (100 to 5000 μm^2) and the uncertainties in aerosol size distribution measurements, an experimental uncertainty of a factor of 3 to 5 is set on the TEM based results.

Particle Size Detailed Deposition Velocities

$$V_{\max} = 305 \text{ cm/sec, } \nu^* = 35 \text{ cm/sec}$$

Particle Diameter D_p (microns)	K_{Dp} (cm/sec) Distribution		\bar{K}_{Dp} (cm/sec)
	I	II	
0.1	0.002	0.001	0.002
0.2	0.0008	0.0008	0.0008
0.4	0.002	0.002	0.002
0.8	0.01	0.03	0.02
1.6	0.03	0.04	0.04
3.2	0.1	—	0.1

analyzed by XPS. A standardization curve (Fig. 8) was constructed by plotting the XPS peak area ratio S_{2p}/Zn_{2p} versus moles of H_2SO_4 for each standardization sample. Identical Zn discs were mounted flush with the walls of the test section of the aerosol flow system and were exposed to measured concentrations of aerosol H_2SO_4 for a measured length of time. The XPS spectra of each of these samples were measured and the S_{2p}/Zn_{2p} peak area ratio was calculated. The number of moles of deposited H_2SO_4 for each sample was taken off the standardization curve. The range where the deposited aerosol test samples fell on the standard curve is also shown in Figure 8. The bulk flux determinations combined with the total filter aerosol mass data were used to calculate the deposition velocities for two frictional velocities. These results, shown in Table 2, were for the aerosol size distribution without the cyclone separator.

The potential for experimental error in determining the size distribution of the particles on the TEM grids, and the small surface area involved in the analyses, leads to an estimated uncertainty in the deposition velocities calculated from the TEM data of about a factor of 3. The bulk deposition velocities obtained from the XPS analyses did involve greater sample sizes and a means of quantitative calibration and provide a more accurate determination. Comparison of the two determinations for $K_{H_2SO_4}$ from Distribution I (Fig. 6) shows the XPS based value to be about 3.5 times greater than that from the TEM data. A comparison between the TEM based detailed deposition velocities and the theoretical values calculated by G. A. Sehmel in 1972(9) from wind tunnel data on uranine particles (density 1.5 gr/cm^3) is shown in Fig. 9. The magnitude of the values for K_{dp} agree quite well considering the uncertainty in the results, and the shape of the profile supports Sehmel's model which predicts a minimum in the deposition velocity for particles in the accumulation mode size range.

The deposition velocities for SO_2 on zinc as determined from XPS measurements were obtained for concentrations of SO_2 between 100 and 200 ppb by volume at flow velocities of 400 cm/sec, corresponding to a frictional velocity of about 50 cm/sec and a roughness height of about 0.2 cm. The results for these conditions gave:

$$K_{SO_2} = 0.93 \pm 0.2 \text{ cm/sec}$$

Typical ambient grassland studies show SO_2 deposition velocities varying from 0.1 to 1.5 cm/sec for frictional velocities 20 to 40 cm/sec(10), and Owen and Powell (1973) report that a K_{SO_2} value of 0.8 cm/sec is an average value over land(11) for the British Isles.

CORROSION MEASUREMENTS

All corrosion measurements were made through the use of the atmospheric corrosion monitor (ACM) described in the experimental section of this report. This unit consisted of 10, zinc-to-zinc anode-cathode couples across which current, (I_g), was monitored by a zero resistance ammeter as a function of time. The polarity of the 30 mv bias voltage was reversed at 1 cycle per minute. As described by Mansfeld(12), the relationship of I_g with the rate

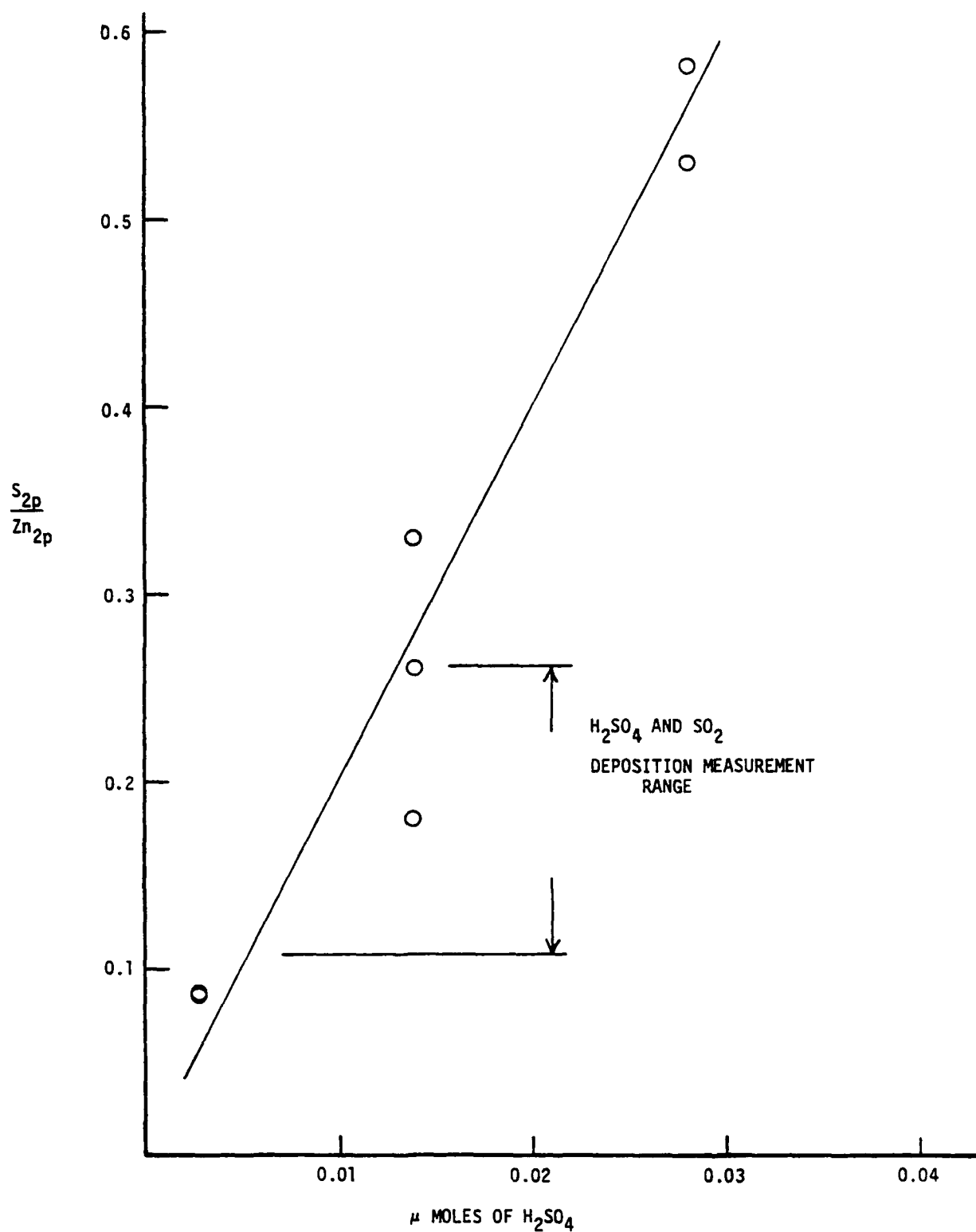


FIGURE 8.. Ratio of integrated XPS S_{2p} signal to integrated XPS Zn_{2p} signal for H_2SO_4 -treated Zn discs (0.242 cm^2 surface area)

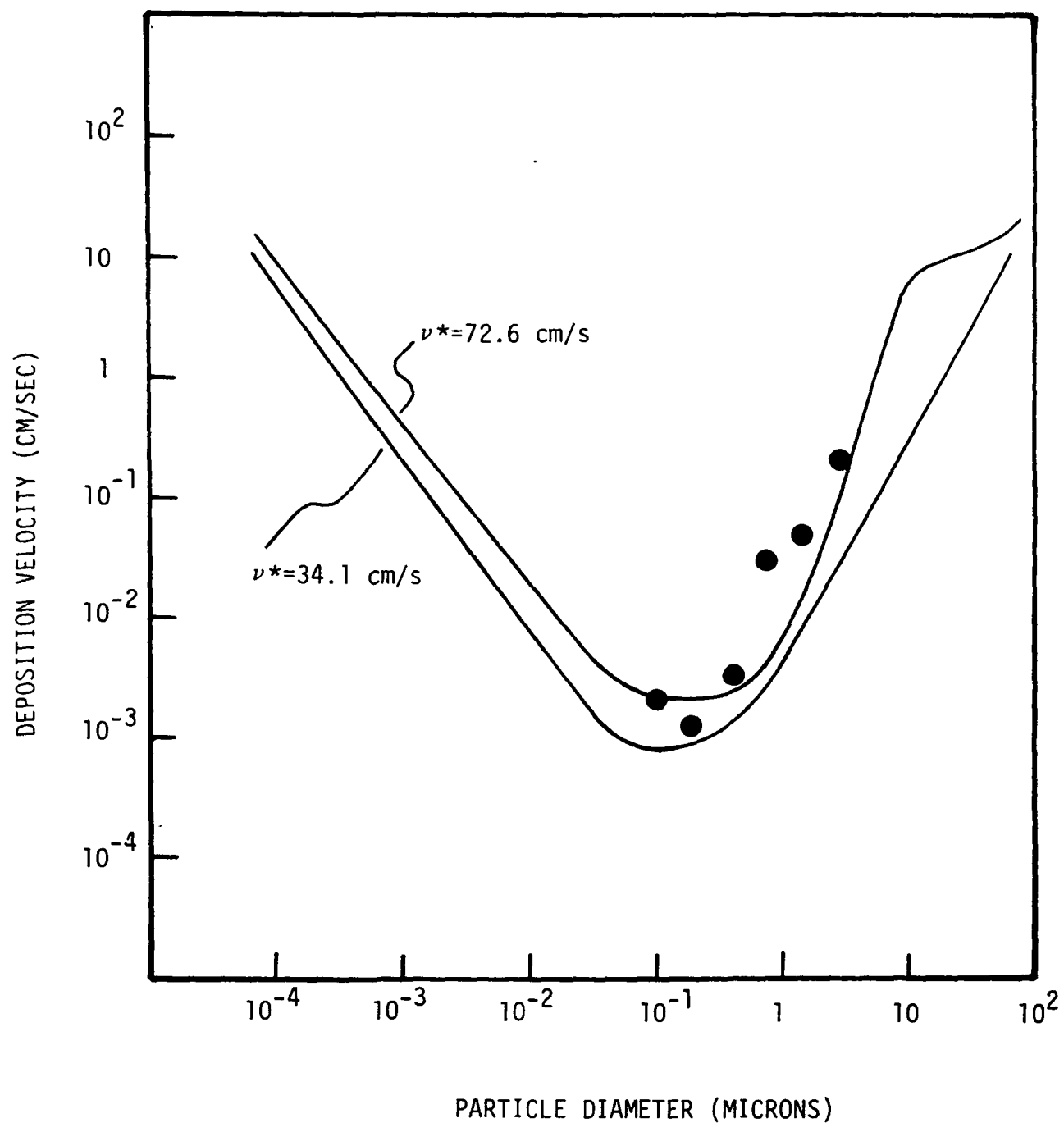


Figure 9. Comparison of experimental aerosol deposition velocities with those predicted by Sehmel (9).

● - Experimental points at frictional velocity $v^* = 35 \text{ cm/s}$

Smooth curves - Theoretical values at $v^* = 72.6 \text{ cm/s}$ and at 34.1 cm/s

of the corrosion process for a theoretical case in which the cathodic reaction is under pure diffusion control is given by

$$I_c = k_c \gamma, \quad (V)$$

where γ is the corrosion rate and k_c a constant. The observed ACM current I_g is related to the actual corrosion current by $I_c = K I_g$ (V), where k is a constant composed of the ratio of Tafel slopes and the polarization resistance. Hence the observed current I_g under controlled conditions should be directly related to the instantaneous corrosion rate. Before each experiment the surface of the ACM unit was mechanically polished on 600 grit corborundum paper and the resistance of the background current in the absence of applied electrolyte determined. The ACM was only used in a test if the observed resistance was greater than $10 \text{ M } \Omega$. The freshly polished ACM surface was then uniformly wetted with 0.7 ml of 0.01 N H_2SO_4 electrolyte and was allowed to dry overnight in an airflow at 60% RH to develop a uniform layer of corrosion products.

Various pretreatment electrolytes were investigated to determine their relative sensitivity to humidity and sulfate deposition. Pretreatment electrolytes studied included deionized water, 0.01 N H_2SO_4 , 0.01 N Na_2SO_4 , and mixtures of 0.01 N HCl and 0.01 N H_2SO_4 . The results of these tests showed that except for the case of deionized water, the surface pretreatment solutions produce equivalent sensitivities when dried under equivalent conditions. The deionized water produced very little corrosion products on the surface of the ACM and very low (10^{-7} amp) current response when cycled by the potentiostat. The other surface pretreatments produced stable current levels at a given level of relative humidity, with the humidity dependence of the current being shown in Figure 10. As can be seen, the data on the $\log I_g$ versus % RH has scatter but gives a fairly linear relationship for all of the pretreatment electrolytes.⁽¹⁴⁾ Since no advantage was found to having Na^+ or Cl^- ions on the ACM surface, 0.01 N H_2SO_4 was selected as the standard pretreatment solution. Under standard test conditions where RH was normally maintained between 85 and 95%, the background corrosion currents due to the surface pretreatment were about 1 microamp.

HIGH-LOW CONDITION TESTS

The experimental design called for a series of "High-Low" tests to be conducted to determine the experimental parameters controlling the Zn corrosion rate. Tests with high and low levels for flow rate, % RH, pollutant concentration, and turbulence established that the primary controlling parameters were relative humidity and pollutant flux.

Relative humidity was, as expected, a dominant variable. At RH levels below the surface wetness point, where the surface corrosion products have established an equilibrium with gaseous H_2O producing a thin electrolyte film on the ACM, no pollutant related current effects were observed. Aerosol droplets falling on the ACM surface were no doubt causing point corrosion effects while drying on the surface, but the absence of an electrolyte film prevented any significant current changes from being observed.

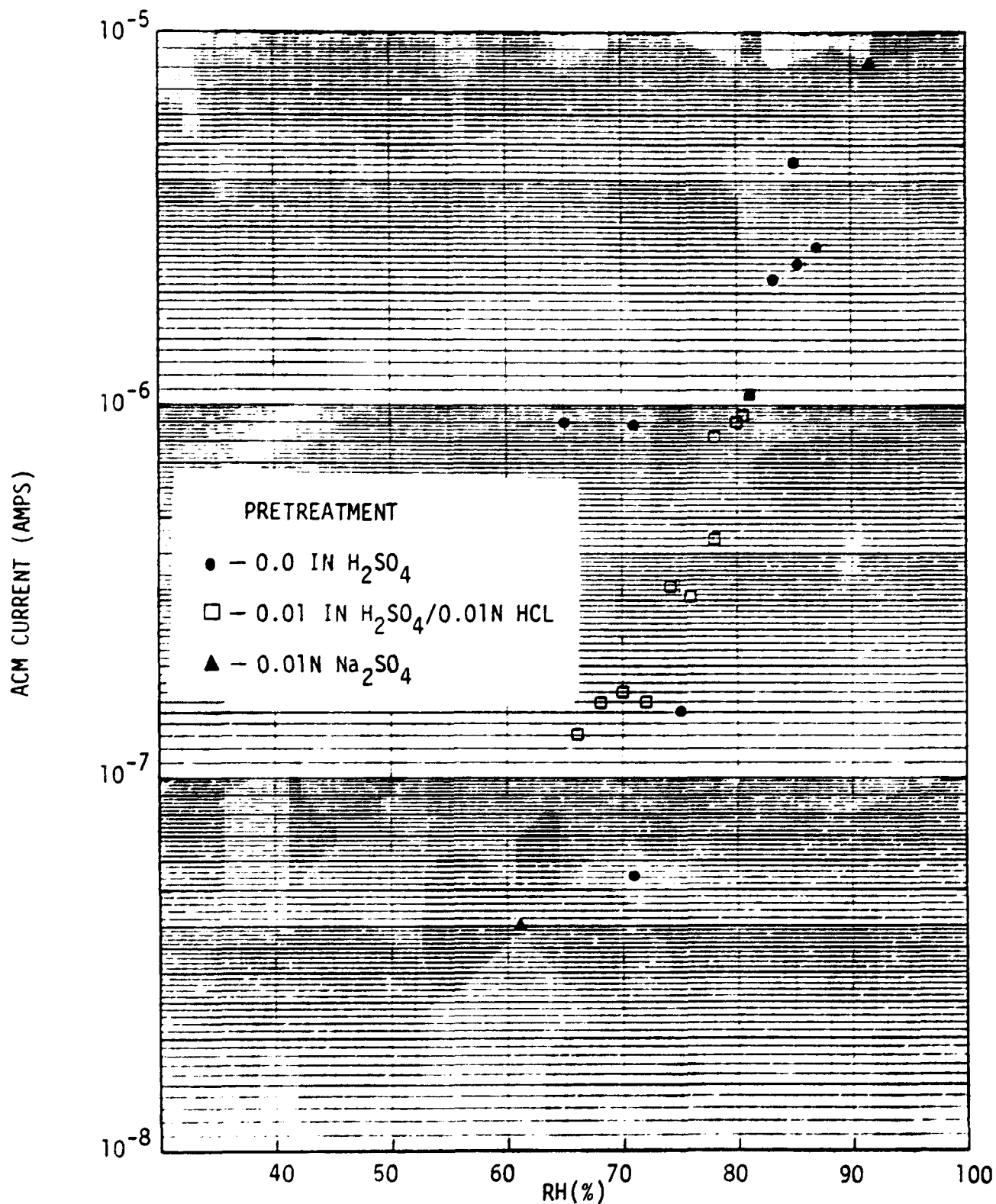


Figure 10. Comparison of the humidity response of the atmospheric corrosion monitor with various surface pre-treatments.

The second controlling feature was the flux of pollutants to the surface. Pollutant concentration and frictional velocity are the two parameters describing pollutant flux, and both were found to have an effect upon the observed corrosion rate.

Pollutant concentration was obviously a controlling factor in that at low pollutant levels (<10 ppb of SO_2), no enhancement of the corrosion current was observed, while at higher levels of SO_2 and H_2SO_4 the corrosion current increased with pollutant concentration. This can be seen in the I_g versus time profiles observed for SO_2 in Figure 11, where both the rate of increase and the magnitude of the current are controlled by the SO_2 level.

That frictional velocity was affecting the corrosion current was more difficult to clearly demonstrate in that over the range of frictional velocities used in the corrosion tests (10 to 75 cm/sec) the total deposition velocity for the accumulation mode aerosols did not change greatly (Table 2). However, as can be seen in Figure 12, there is an observable increase in the corrosion current between the two test runs at $\nu^* = 30$ and $\nu^* = 50$ for comparable aerosol concentrations and % RH.

NH_4HSO_4 AEROSOL GENERATION:

The ACM measurements demonstrated that under RH conditions where the ACM surface had established a thin layer of electrolyte corrosion rate enhancement due to SO_2 and H_2SO_4 surface deposition could be observed. The test runs using NH_4HSO_4 aerosol did not produce any corrosion current increase. Investigation of the aerosol size distribution and concentration showed that the saturated solution of NH_4HSO_4 , though generating a large initial concentration of aerosols, was not producing high aerosol levels in the flow system. A check of the flow system showed that the aerosols were rapidly agglomerating and forming salt crystals in the aerosol inlet tubes, allowing only small concentrations of aerosols to enter the flow tube.

Examining the literature on generation methods for NH_4HSO_4 aerosols revealed that other studies had also encountered difficulties in generating the ammonium acid sulfate aerosols. An extensive study by R. Zygmunt⁽¹³⁾ showed that the bisulfate aerosols react in air to form other sulfate forms including letovicite, $(\text{HN}_4)_3\text{H}(\text{SO}_4)_2$, and ammonium sulfate, $(\text{NH}_4)_2\text{SO}_4$. The combination of the agglomeration phenomena and the neutralization of the aerosols while airborne discouraged any further tests with these aerosols.

CORROSION CHEMISTRY

The ACM current, I_g , observed during the SO_2 and H_2SO_4 exposure experiments showed different time profiles for the two pollutants as can be seen in Figures 11 and 12. The SO_2 exposure experiments showed the current to build up towards a maximum limit, while H_2SO_4 exposure produced a more linear monotonic increase in I_g as a function of time. In both cases when the pollutant flow was discontinued the ACM current dropped back towards a baseline value indicating that the sulfur pollutants reacted to completion. XPS analysis of the chemical composition of the surface corrosion layer produced

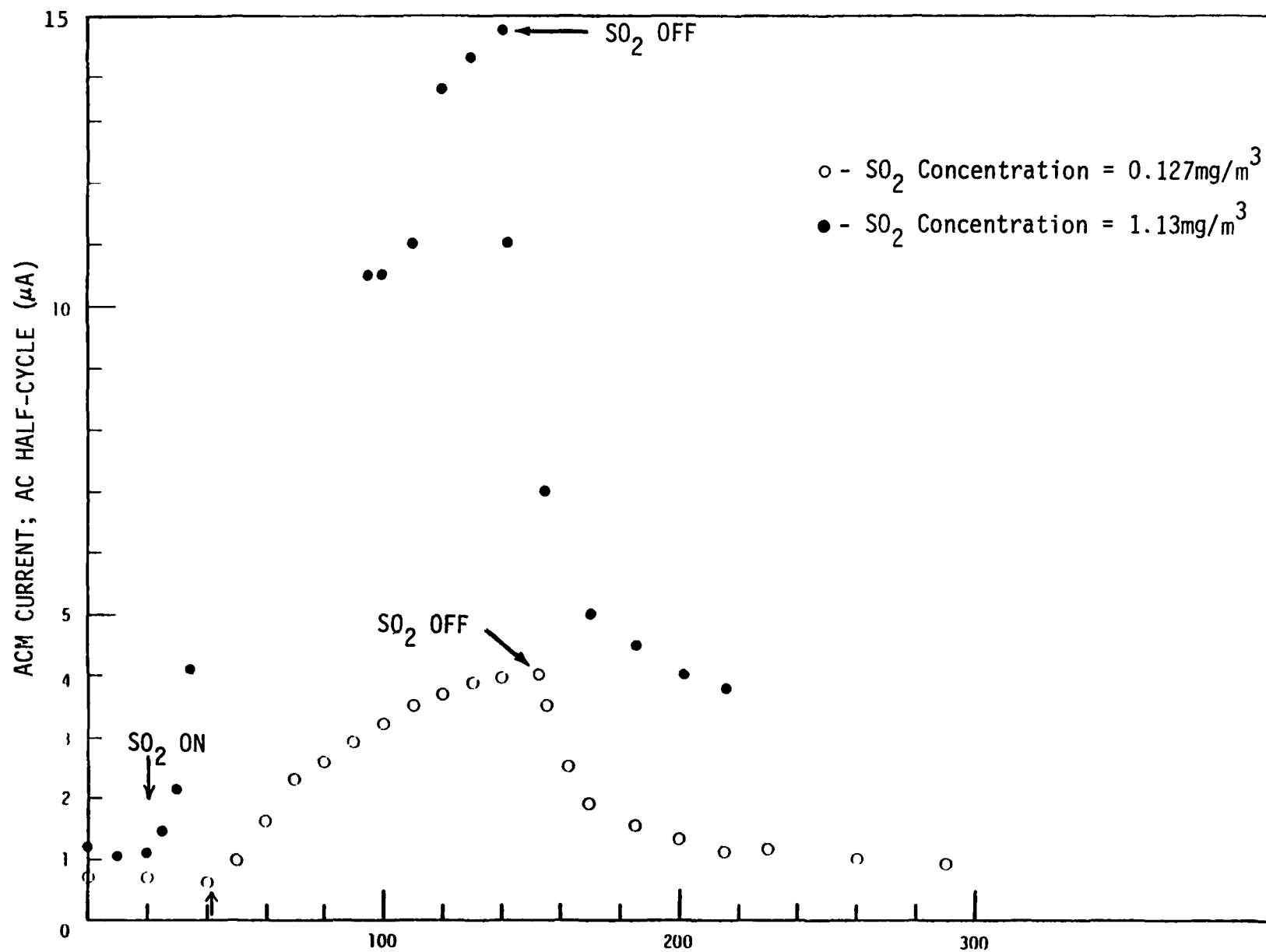


Figure 11. Output current of Atmospheric Corrosion Monitor as a function of SO₂ Concentration. Arrows indicate the respective start and stop times of SO₂ flow for each experiment.

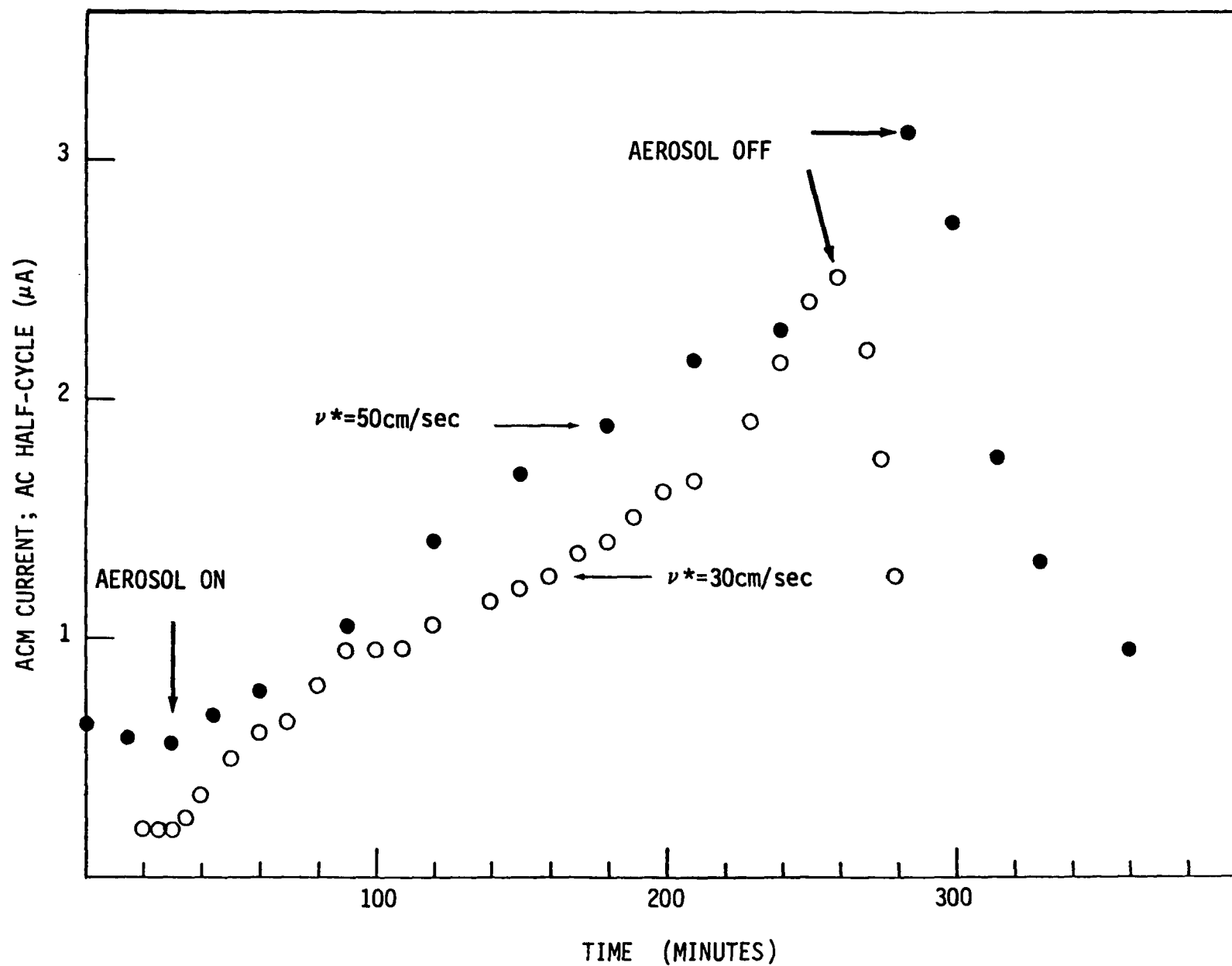


Figure 12. Comparison of observed ACM current response to H_2SO_4 aerosol deposition at two frictional velocities. H_2SO_4 concentration = 3.2 mg/m^3 .

by exposure to SO_2 and H_2SO_4 showed that in both cases the surface reactions lead to the formation of zinc sulfate. The XPS spectra showed all the surface Zn to be in the Zn^{2+} state with SO_4^{2-} being the only form of sulfur on the surface.

Since in the examples shown in Figure 11 and 12 the deposition rate of SO_2 is a factor of two greater than that for H_2SO_4 and I_g for SO_2 was approaching a steady-state limit more rapidly than the H_2SO_4 , it is reasonable to assume that the SO_2 was reacting more rapidly in the surface electrolyte than the sulfuric acid. The steady increase in the H_2SO_4 induced current with time indicates that the reaction was proceeding at a rate slow enough such that the concentration of sulfuric acid in the surface electrolyte was continuously building up. Further insight into the rates of the two reaction mechanisms can be obtained from the half-life of the decay of the observed ACM current when the pollutant flow was turned off. The average of all the observed cases showed the SO_2 induced current to drop to one half of its maximum value above the base line in 15 ± 1 minutes, while the H_2SO_4 case required 30 ± 9 minutes.

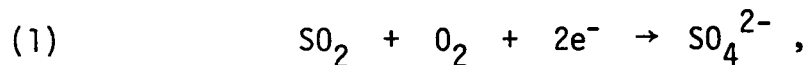
If as suggested by equation (V) the observed ACM current is directly related to the instantaneous corrosion rate, the area under the I_g versus time profiles normalized for the deposition of pollutants should provide a means of comparing the relative number of electrons involved in the SO_2 and H_2SO_4 induced corrosion processes. The average of this total charge value for two SO_2 tests and three H_2SO_4 tests run under identical flow dynamic conditions, using the bulk XPS deposition velocities for normalization, yielded

$$\text{Total Charge } \text{SO}_2 = 3.64 \pm 0.8 \times 10^4 \text{ coulombs/mole}$$

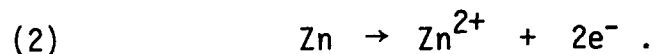
$$\text{Total Charge } \text{H}_2\text{SO}_4 = 4.6 \pm 1.5 \times 10^4 \text{ coulombs/mole.}$$

These total charge values are consistent with the two reaction mechanisms involving the transfer of the same number of electrons between the zinc metal and the electrolyte; however the experimental uncertainty in the deposition velocity values prevents any conclusive statement.

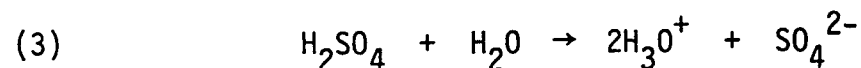
The SO_2 adsorbed into the surface electrolyte was ultimately converted to sulfate, hence the net reaction would be

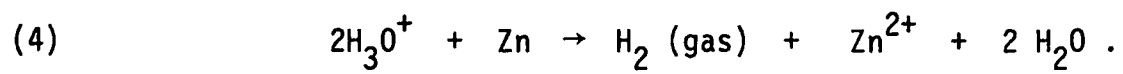


where the zinc metal could supply the electrons and the observed ACM current through



The reaction of the sulfuric acid aerosols with the zinc would be expected to proceed through the liberation of gaseous hydrogen as shown by





SECTION 4

DISCUSSION OF RESULTS

The results of this study confirm that the principal factors controlling the rate of sulfur pollutant induced corrosion of zinc are relative humidity, pollutant flux to the surface, and the chemical form of the pollutant. No corrosion was observed to proceed on the zinc surfaces at relative humidities below that required to establish a layer of electrolyte, while at RH levels high enough to produce a "wet" surface the corrosion rate was primarily a function of the concentration of the sulfur pollutant in the thin electrolyte layer and the chemical nature of the pollutant. The results indicate that SO_2 induced corrosion of zinc proceeds at a rate approximately a factor of two greater than that for the equivalent amount of deposited sulfuric acid aerosol while ammonium bi-sulfate induced corrosion was not observed for the levels of aerosols generated in this study. The experimental data also supports chemical mechanisms for the SO_2 and H_2SO_4 induced corrosion of zinc which involve the same number of electrons being transferred from the zinc metal per molecule of pollutant.

The flow dynamics data provided a measurement of the particle size dependence of the accumulation mode aerosols at 35 cm/sec frictional velocity which support the general theoretical treatment of Sehmel⁽⁹⁾ showing atmospheric deposition velocities to be at a minimum for aerosol particles in this size range (0.1 to 1.0 micron diameter). The aerosol deposition measurements showed the two experimental accumulation mode aerosol size distributions to have bulk deposition velocities of less than 10^{-1} cm sec⁻¹ at a ν^* of 35 cm sec⁻¹ versus the 0.9 cm sec⁻¹ value observed for SO_2 at a frictional velocity of $\nu^* = 50$ cm sec⁻¹. These deposition velocities can be used with ambient levels of SO_2 and H_2SO_4 aerosols to obtain an approximate assessment of their relative contribution to zinc corrosion.

As an example, the Los Angeles basin in the summer and early fall months has SO_2 levels ranging from 1 to 100 ppb by volume with a typical level for an hourly average being around 20 ppb. During the same period, background levels of 10 to 20 $\mu\text{g}/\text{m}^3$ of SO_4^{2-} are normal. Using 20 ppb of SO_2 and 15 $\mu\text{g}/\text{m}^3$ of SO_4^{2-} as H_2SO_4 (though much of the SO_4^{2-} would be in the form of ammonium sulfate) the experimental deposition velocities predict deposition rates of $0.18 \mu\text{g cm}^{-2} \text{ hr}^{-1}$ for SO_2 and $<0.006 \mu\text{g cm}^{-2} \text{ hr}^{-1}$ for H_2SO_4 aerosols on a horizontal surface. The actual relative contribution of these pollutants to enhanced materials damage will of course be a direct function of the ambient conditions in a given area. However, it appears that SO_2 induced damage will dominate over H_2SO_4 effects in most urban areas.

In order to quantitatively relate the observed ACM current to the actual

corrosion rates and to assess the combined effects of various pollutants on the corrosion of ambient materials, further experimental efforts will be required. The experimental technique developed throughout this study has shown itself capable of observing both the physical and chemical variables controlling pollutant induced corrosion and offers a unique means of developing an in-depth understanding of this area through continued research.

REFERENCES

1. Robinson, E., and R. C. Robbins, Sources, Abundance, and Fate of Gaseous Atmospheric Pollutants. Stanford Research Institute, Menlo Park, CA, Project PR-6755, prepared for American Petroleum Institute, New York, N.Y. (Feb. 1968).
2. Charlson, R. J., D. S. Covert, T. V. Larson and A. P. Waggoner. Chemical Properties of Tropospheric Sulfur Aerosols. *Atm. Environ.* 12 pp 39-53 (1978).
3. Friend, J. P. The Global Sulfur Cycle. *Chemistry of the Lower Atmosphere*. Ed. S. I. Rasool (Plenum Press, N.Y., N.Y., 1973) pp 177-201.
4. Whitby, K. T. The Aerosol Size Distribution of Los Angeles Smog. *J. Colloid Interface Sci.* 39, pp 177-204 (1972).
5. Position Paper on Regulation of Atmospheric Sulfates. EPA-450/2-75-007. U.S. Environmental Protection Agency, Research Triangle Park, N.C. pp 2, 13, 22-24, 27-34, 36 (Sept. 1975).
6. Mansfeld, F. and J. V. Kenkel. Electrochemical Monitoring of Atmospheric Corrosion Phenomena. *Corrosion Science.* 16, pp 111-122 (1976).
7. Mansfeld, F. B. Electrochemical Studies of Atmospheric Corrosion. Final Report Contract No. N00014-75-C-0788 prepared for Office of Naval Research (1979).
8. Owers, E. and R. C. Pankhurst. The Measurement of Air Flow. Pergamon Press, N.Y., N.Y. 1977) pp 77.
9. Sehmel, G. A. Particle Eddy Diffusivities and Deposition Velocities For Isothermal Flow and Smooth Surfaces. *Aerosol Science.* 4, pp 125-138 (1973).
10. Proceedings of the International Symposium on Sulfur in the Atmosphere. Held in Dubrovnik, Yugoslavia September 7-14, 1977. Published in *Atmos. Environ.* 12, pp 14 (1978).
11. Owers, M. J. and A. W. Powell. Deposition Velocity of Sulfur Dioxide on Land and Water Surfaces Using a ³⁵S Tracer Method. *Atmos. Environ.* 8, pp 63-67 (1974).
12. Mansfeld, F. and J. V. Kenkel. Electrochemical Measurements of Time-of-Wetness and Atmospheric Corrosion Rates. *Corrosion* 33, pp 13-16 (1977).
13. Zygmunt, R. W. A Study of the Production of Well-Characterized Aerosols Using a Flow Reactor. Argonne National Lab report #ANL-77-90, (1977).
14. Mansfeld, F. and J. V. Kenkel. Atmospheric Corrosion Rates, Time-of-Wetness and Relative Humidity. *Werkstoffe und Korrosion.* 30, 38 (1979).

TECHNICAL REPORT DATA <i>(Please read instructions on the reverse before completing)</i>		
1. REPORT NO. EPA-600/3-80-018	2.	3. RECIPIENT'S ACCESSION NO.
4. TITLE AND SUBTITLE MECHANISM OF SO ₂ AND H ₂ SO ₄ AEROSOL ZINC CORROSION		5. REPORT DATE January 1980
		6. PERFORMING ORGANIZATION CODE
7. AUTHOR(S) Alan B. Harker, Florian B. Mansfeld, Dennis R. Strauss and Dwight D. Landis		8. PERFORMING ORGANIZATION REPORT NO.
9. PERFORMING ORGANIZATION NAME AND ADDRESS Rockwell International Science Center Thousand Oaks, CA 91360		10. PROGRAM ELEMENT NO. 1AA603A AE-029 (FY-79)
		11. CONTRACT/GRANT NO. 68-02-2944
12. SPONSORING AGENCY NAME AND ADDRESS Environmental Sciences Research Laboratory--RTP, NC Office of Research and Development U.S. Environmental Protection Agency Research Triangle Park, NC 27711		13. TYPE OF REPORT AND PERIOD COVERED Final 5/9/79-6/9/79
		14. SPONSORING AGENCY CODE EPA/600/09
15. SUPPLEMENTARY NOTES		
16. ABSTRACT This study established the physical variables controlling the SO ₂ and H ₂ SO ₄ induced corrosion of zinc. Relative humidity, temperature, air flow velocity, flow turbulence, aerosol size range, and pollutant concentration were controlled. Corrosion measurements were made through the use of an atmospheric corrosion monitor. The results showed that the principal factors controlling pollutant induced corrosion are relative humidity, the rate of pollutant flux to the surface, and the chemical form of the pollutant. SO ₂ was observed to induce a higher corrosion rate in the zinc than H ₂ SO ₄ on a molecule for molecule basis. Flow dynamic measurements provided bulk and size detailed deposition velocities for two different accumulation mode H ₂ SO ₄ aerosol size distributions as a function of frictional velocity, and a deposition velocity for SO ₂ gas. The overall results indicate that under most ambient conditions SO ₂ induced corrosion damage will dominate over H ₂ SO ₄ effects.		
17. KEY WORDS AND DOCUMENT ANALYSIS		
a. DESCRIPTORS	b. IDENTIFIERS/OPEN ENDED TERMS	c. COSATI Field/Group
*Air pollution *Aerosols *Sulfur dioxide *Sulfuric acid *Zinc *Corrosion mechanisms		13B 07D 07B 11M
18. DISTRIBUTION STATEMENT RELEASE TO PUBLIC	19. SECURITY CLASS (This Report) UNCLASSIFIED	21. NO. OF PAGES 41
	20. SECURITY CLASS (This page) UNCLASSIFIED	22. PRICE